JMEPEG (2011) 20:120–132
DOI: 10.1007/s11665-010-9658-5

1059-9495/$19.00

Energy Efficient Heat Treatment for Linerless Hypereutectic Al-Si Engine Blocks Made Using Vacuum HPDC Process

W. Kasprzak, J.H. Sokolowski, H. Yamagata, M. Aniolek, and H. Kurita

(Submitted February 28, 2009; in revised form February 6, 2010)

Heat treatment standards developed by the aluminum industry over the last several decades are often not well optimized when applied to components cast by high cooling rate processes such as High Pressure Die Casting (HPDC), Low Pressure Permanent Mold (LPPM), Squeeze Casting, etc. The inherently finer as-cast structures should not require long solution times for the effective dissolution of intermetallic phases and the adequate thermal modification of structural constituents. Hence, long and expensive T6 and T7 treatments should not be required. Heat treatment studies involving as-cast laboratory samples with SDAS = 13.6 μm (equivalent to a thick-section HPDC casting) were conducted. Traditional and modified solution and aging treatments were compared. These studies suggest that a reduction of up to 92% in thermal processing time is possible while maintaining and/or improving the cast component's metallurgical characteristics including hardness (≥75 HRB), dissolution of secondary phases, and spheroidization of the eutectic Si as well as overall homogeneity. Vacuum HPDC of an actual hypereutectic Al-20%Si motorcycle engine block confirmed the potential for significantly reduced heat treatment times, energy consumption, and overall costs.

Keywords Al-Si hypereutectic alloy, heat treatment, non-equilibrium thermal analysis, physical simulations of metallurgical processes, primary Si, secondary dendrite arm spacing, vacuum High Pressure Die Casting (HPDC)

1. Introduction

Hypereutectic Al-Si alloys are recognized as excellent materials for high performance cast components that are desired in transportation powertrain applications. The combination of excellent wear resistance, thermal conductivity, and weight reduction make these materials good candidates for linerless engine block applications (Ref 1-5). In particular, the higher Si concentration in hypereutectic alloys minimizes thermal expansion while increasing the alloy's thermal conductivity thus simultaneously improving engine cooling performance and reducing oil consumption (Ref 1, 4, 6). The tribological properties are mainly controlled by the primary Si crystal size, distribution, and exposure height from the aluminum matrix (Ref 7, 8). The macrohardness of heat-treated hypereutectic alloys is predominately determined by the volume fraction of primary and eutectic Si phases in addition to the hardness of the aluminum matrix controlled largely by Cu (or other elements) via precipitation strengthening (Ref 3, 4, 7). Adequate refinement of the primary Si crystals is of key importance and creates a technological challenge particularly for slowly solidified cast components. Currently, the R&D focus is on the modification of the primary Si crystals and other structural constituents as well as grain size refinement that can be achieved by controlled alloying, optimized management of the melt preheating and pouring temperatures, rapid solidification, electromagnetic, and ultrasonic melt treatment techniques (Ref 2, 5, 9-12).

W. Kasprzak and **M. Aniolek**, CANMET Materials Technology Laboratory, 568 Booth Street, Ottawa, ON K1A 0G1, Canada; **J.H. Sokolowski**, Light Metals Casting Technology Group, Department of Mechanical, Automotive and Materials Engineering, University of Windsor, Room 218, Essex Hall, 401 Sunset Avenue, Windsor, ON N9B 3P4, Canada; **H. Yamagata**, Gifu University, Centre for Advanced Die and Mold Engineering, 1-1 Yanagido, Gifu 501-1193, Japan; and **H. Kurita**, R&D Operations, Yamaha Motor Co. Ltd., 2500 Shingai, Iwata, Shizuoka 438-8501, Japan. Contact e-mail: wkasprza@nrcan.gc.ca.

Advanced motorcycle engine blocks are manufactured using vacuum-assisted High Pressure Die Casting (HPDC) (Ref 4, 7). Properly applied, this technology renders improved structure, mechanical, and functional characteristics. Conventional HPDC components are not easily solution treated because of air entrapment during rapid mold filling resulting in blistering. Recent progress in the vacuum-assisted HPDC technology minimizes gas content and allows for high temperature solution treatment resulting in further improvement of the mechanical properties (Ref 4, 7).

Proper design of heat treatment operations is crucial to obtain the required casting properties and therefore has been given considerable research attention (Ref 6, 13-27). The high temperature solution treatment operation goes beyond the 480 to 495 °C temperature range that is used for conventional solution treatment and therefore significantly improves the dissolution kinetics of the intermetallic phases, improves eutectic Si thermal modification as well as contributes to the strengthening of the aluminum matrix during the artificial aging operation (Ref 13, 17, 25). In turn, mechanical properties (including fatigue—for cast component(s) free of porosity) could be controlled and optimized by proper selection of the heat treatment processing parameters. For high integrity castings, fatigue performance is affected by the brittle phases, their cohesiveness with the aluminum matrix and the mechanical properties of the matrix (Ref 4, 6).

The existing heat treatment standards were designed predominantly for sand cast components with coarse microstructures characteristic of slow cooling rates. Rapid solidification of the permanent mold cast components results in an elevated solute content in the as-cast condition. Cooling rates during solidification for LPPM and HPDC processes typically range from >10 to ~100 °C/s, respectively. In contrast, sand castings solidify at an average solidification rate lower than 5 °C/s (Ref 2, 9). Thermal analysis data indicate that slow reheating of the rapidly solidified test samples results in solid state exothermic reaction(s). Therefore, the elevated solute content in the metal matrix is used for subsequent alloy hardening during the natural aging and/or artificial aging operations. Such highly non-equilibrium casting microstructures could allow for application of the T5 operation and might eliminate long and expensive solution treatment processes conventionally used for the T6 and T7 treatments. Consequently, heat treatment cycle reduction will lead to significant energy savings while delivering good mechanical and tribological properties.

The capabilities of the Universal Metallurgical Simulator and Analyzer UMSA (Ref 28) enable the replication of industrial casting process, together with semi-continuous heat treatment processes such as heat treatment after casting ejection. Utilization of conventional laboratory steel molds cannot ensure as-cast structures that are fully representative of the specific cast component sections that are of research and applied engineering interest (Ref 9, 27).

The presented research has three main objectives: to demonstrate the possibility of a significant reduction of the heat treatment duration for the rapidly solidified HPDC engine block while: (i) maintaining the presently achievable HRB hardness of approximately 73 and (ii) exceeding the hardness of 75 HRB of the cylinder bore wall as well as (iii) utilizing the heat treatment test samples for future research aimed at correlating the tribological characteristics with other materials' properties (including fatigue and cohesiveness as well as macro and microhardness).

2. Experimental Procedures

2.1 Alloy Chemistry and Test Sample Design

The Al-20%Si alloy's chemical composition listed in Table 1 was used in the present studies. This phosphorus modified alloy was specifically developed for the vacuum-assisted HPDC technology used to manufacture the linerless motorcycle engines blocks (Ref 7) (Fig. 1). The P addition helps achieve uniform size, shape, and distribution of the primary Si crystals nucleated by AlP_3 particles during solidification (Ref 9). Mg lowers the solidus temperature and forms a ternary eutectic with Cu and Al at the end of solidification while increasing alloy strength and hardness in the heat treated condition by precipitation strengthening of the Mg_2Si phase (Ref 6).

In order to closely simulate the engine block cylinder bore geometry's ring shape, UMSA samples with an outer diameter of 44.7 mm, an inner diameter of 35.4 mm, and a height of 12 mm were machined out from the Al-20%Si phosphorus modified ingot. The test sample wall thickness was ~5 mm, corresponding to the thickness of the engine block cylinder bore wall, Fig. 1. The representative micrograph of the cylinder bore microstructure is presented in Fig. 2. In order to maintain

Table 1 Average chemical composition of the hypereutectic Al-20%Si ingots (wt.%) used for vacuum HPDC engine block castings and UMSA test samples

Si	Cu	Mg	Zn	Fe	Mn	Ni	Ti	P
20.0	3.0	0.5	0.1	0.5	0.1	0.1	0.001	0.01

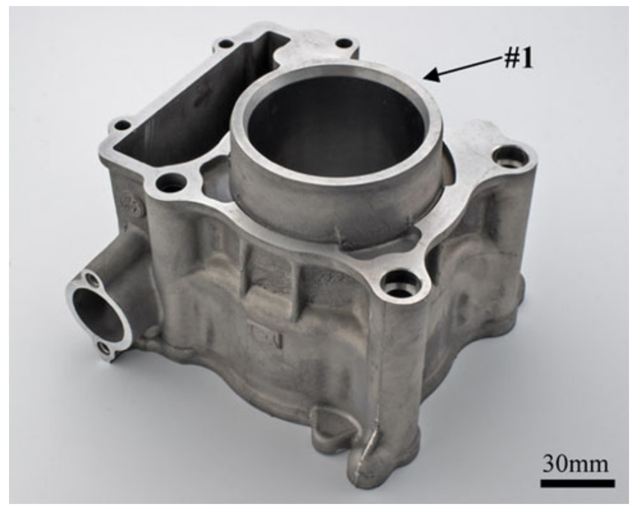

Fig. 1 Overall view of the Al-20%Si engine block cast using the vacuum-assisted HPDC process. The hardness after the conventional T6C#9 heat treatment (solution at 490 °C for 4 h and aging at 200 °C for 4 h) measured at the bore wall (#1) is 73.5 ± 1.7 HRB

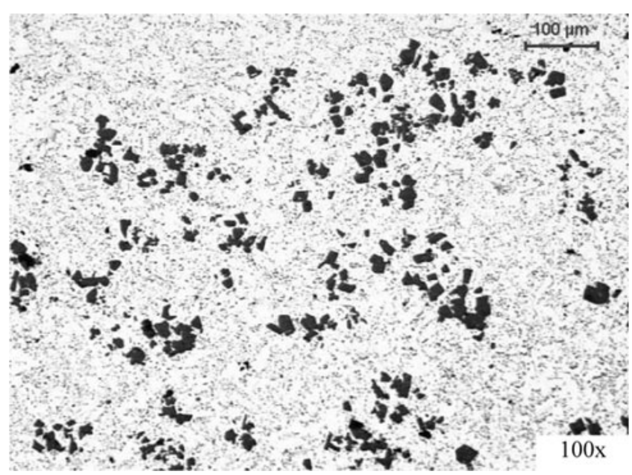

Fig. 2 Optical micrograph (100×) of the Al-20%Si phosphorous modified HPDC engine block's cylinder bore section after the conventional T6C#9 heat treatment (solution at 490 °C for 4 h and aging at 200 °C for 4 h). ED of the primary Si particles is approximately 25 µm and average SDAS varies between 5 and 8 µm. Note the low level tendency of primary Si particles to agglomeration

a high level of experimental reproducibility and precision, the test sample mass was kept within a range of 18 ± 0.2 g. Samples were formed in crucibles of 0.25 mm thick stainless steel foil held in place at top and bottom by grooves in the ceramic insulators. Figure 3(a) and (b) shows the crucible components along with a representative test sample before and after assembly and prior to installation in the UMSA Platform. This design considerably reduces thermal inertia and improves the resolution of the thermal analysis signal. Each test sample had a predrilled hole to accommodate a low thermal mass K-type thermocouple. After the re-melting cycle, the metallurgically embedded thermocouple collected in situ thermal data facilitating precise UMSA control of heating and cooling rates. The size of the macro test sample was sufficient for subsequent metallographic analysis as well as selected mechanical testing (i.e., hardness).

2.2 Alloy Thermal Analysis Assessment Prior to the Heat Treatment Experiments

Thermal analysis during the melting and solidification cycles was carried out using the UMSA Technology Platform (Ref 28) (Fig. 4). This Platform allows for the performance of controlled melting, solidification, and heat treatment experiments for the stationary test sample together with advanced thermal analysis of these processes. The heating source is based on high frequency induction heating. The cooling operations are executed using compressed gases, water as well as mist. This Platform allows one to vary the temperature of a test sample as well as the test sample environment (vacuum, inert/active gas, etc.) according to a pre-programmed sequence. Moreover, it is feasible to assess the effects of input variables like temperature, time, cooling rate, etc. on output data including component structure and mechanical properties. Low thermal inertia of the "test sample system" allows for a quick test sample response to the pre-programmed processing parameters thus minimizing overshooting and improving accuracy.

The experiments were performed using ring shaped test samples as described in Section 2.1 and prepared by heating at a rate of approximately 0.75 °C/s to 785 ± 0.2 °C, and held isothermally for a period of 10 min in order to achieve

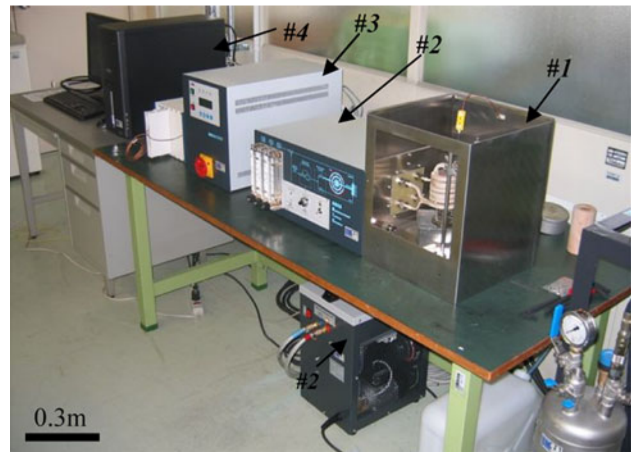

Fig. 4 Universal Metallurgical Simulator and Analyzer UMSA (Ref 28) used for thermal analysis and advanced heat treatment experiments (courtesy of Yamaha Motor Co. Ltd. in Japan). The main system's components are as follows: #1: Testing chamber, #2: Control unit, #3: Induction heating power supplier, and #4: Computer and data acquisition unit

Fig. 3 (a) Customized crucible components shown with representative sample (far right) prior to assembly. Note the 0.25 mm thick stainless steel foil which forms the outside diameter of the sample. This exemplary crucible design is used for a variety of melting, solidification, and heat treatment experiments. (b) Fully assembled UMSA test sample used for advanced heat treatment experiments

homogeneity. The heating rate employed was calculated between 504 °C, the non-equilibrium solidus (start of the melting process), and 711 °C the non-equilibrium liquidus (end of the melting process). Next, the test samples were solidified at a cooling rate of approximately 1 °C/s. After completion of the experimental cycle(s), the temperature versus time was measured, and the corresponding first derivative versus temperature curves were automatically calculated and plotted.

2.3 Selection of the As-Cast Microstructure for the Heat Treatment Experiments

Prior to heat treatment experiments, the cooling rates of UMSA test samples were varied from approximately 1 to 80 °C/s. The temperature signal was recorded at a 20 Hz acquisition rate using a National Instruments data logger integrated with the UMSA Platform. The wide range of cooling rates was achieved by a computer controlled flow of compressed Helium and atomized water (Ref 2, 9, 28, 29). Experimental test samples were subjected to an average cooling rate of approximately 20 °C/s representing the melt temperature upon ladling into the HPDC machine (730 °C) and ejection of the solidified as-cast engine block (380 °C). Test sample microstructures were quantitatively compared with the HPDC motorcycle engine block's cylinder bore and other thick sections using a Leica image analysis system.

Test samples having a Secondary Dendrite Arm Spacing (SDAS) = 13.6 ± 2.6 μm and an Equivalent Diameter (ED) of primary Si crystals of 50 μm were chosen for the heat treatment optimization experiments. The test samples' structural characteristics were identical to the HPDC engine block's thicker sections. Any structural improvements to these sections will be further enhanced for the cylinder bore section that has a SDAS = 5-8 μm and a primary Si ED = 25 μm as explained in Section 3.1.

2.4 Optimization of the Heat Treatment Parameters for the Modified T6, T7, T4, and the T5 Experiments

As-cast test samples having a SDAS = 13.6 ± 2.6 μm experimentally determined by the UMSA-applied cooling rate were subjected to various heat treatment schedules. Figure 5 illustrates the characteristic microstructure while some of the heat treatment schedules are presented schematically in Fig. 6(a-d). Table 2 provides complementary experimental details.

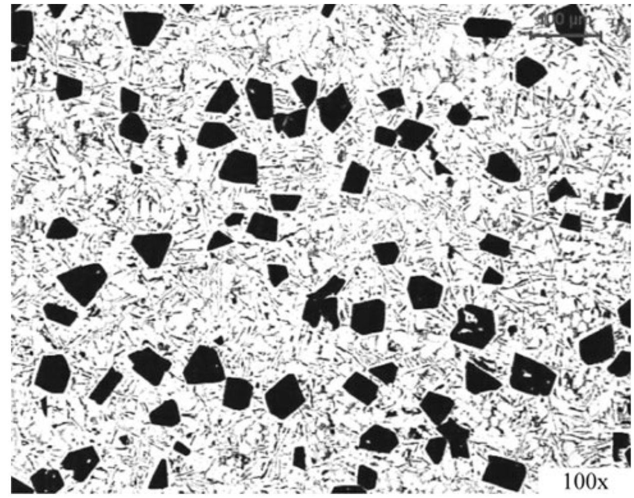

Fig. 5 Optical micrograph (100×) of the Al-20%Si alloy UMSA test sample solidified at an average cooling rate of approximately 20 °C/s. The average ED of primary Si particles is approximately 50 μm and SDAS is 13.6 ± 2.6 μm. This microstructure represents a thick section of the HPDC engine block. Note the uniform distribution of the primary Si particles

Based on the thermal analysis data from the heating cycle (Fig. 7), the solution treatment temperatures were set at 500 and 510 °C while the solution time was chosen to be 0.5 and 4 h. Artificial aging was performed at 200 and 240 °C for 0.5, 2, and 4 h to evaluate the Al-20%Si alloy's response under the modified T4M, T6M, and T7M conditions. Previous studies conducted with 319 alloy having similar concentrations of Cu and Mg at (3.4%) and (0.3%), respectively, suggested that a solution treatment at 510 °C for 0.5 h was optimum for hardness as well as dissolution of Cu-, Mg-based phases. Extending the solution treatment process time above 4 h at 510 °C was not economically justified because this increased the alloy hardness by only three divisions (HV25) and did not cause significant thermal modification of the Al-Si eutectic (Ref 27). After solution treatment, gas quenching under 5 bar compressed air was performed. The average quenching rate was 5 °C/s and should ensure satisfactory casting hardness and strength (Ref 22). All test samples were heated to the solution and the aging temperature at a 0.2 °C/s heating rate. The test sample temperature during the solution treatment and artificial aging operations was kept at ±0.2 °C accuracy. For reference purposes the conventional T6C heat treatment was performed under the following conditions: solution at 490 °C for 4 h followed by gas quenching to room temperature followed by aging at 200 °C for 4 h (Fig. 6d, Table 2 experiment 9).

The modified T6M cycles consist of the solidification process arrested at 380 °C, re-heating to the solution temperature performed at 500 and 510 °C for 0.5 and 4 h followed by interrupted quenching to the aging temperature of 200 °C and a duration time of 4 and 2 h (Fig. 6a, Table 2 experiments 1 to 5). The interrupted quenching schedule might reduce the residual stress level particularly for complex shape castings.

The modified T4M heat treatment was performed for selected test samples as schematically shown in Fig. 6(b). The solidification process was arrested at 380 °C followed by re-heating to the solution temperature of 510 °C and holding for 0.5 h followed by gas quenching to room temperature and natural aging at room temperature for a period of 4 days (Fig. 6b, Table 2 experiment 7).

The modified T5M heat treatment experiments (Fig. 6c, Table 2 experiment 8) were performed to determine the hardness development after the simplified heat treatment operation where the solution treatment was eliminated. Solidifying test samples were quenched when the temperature reached 380 °C. Quenching was accomplished by spraying atomized water under 8 bars of pressure on the test sample's circumference. The water quenching rate was approximately 50 °C/s as estimated by the in situ temperature measurements. Next, the test sample was subjected to aging at 200 °C for 2 h followed by slow cooling to room temperature.

The modified T7M (Table 2 experiment 6) treatment is schematically similar to the modified T6M operation; however, the over-aging temperature was increased to 240 °C, while aging time was shortened to 0.5 h.

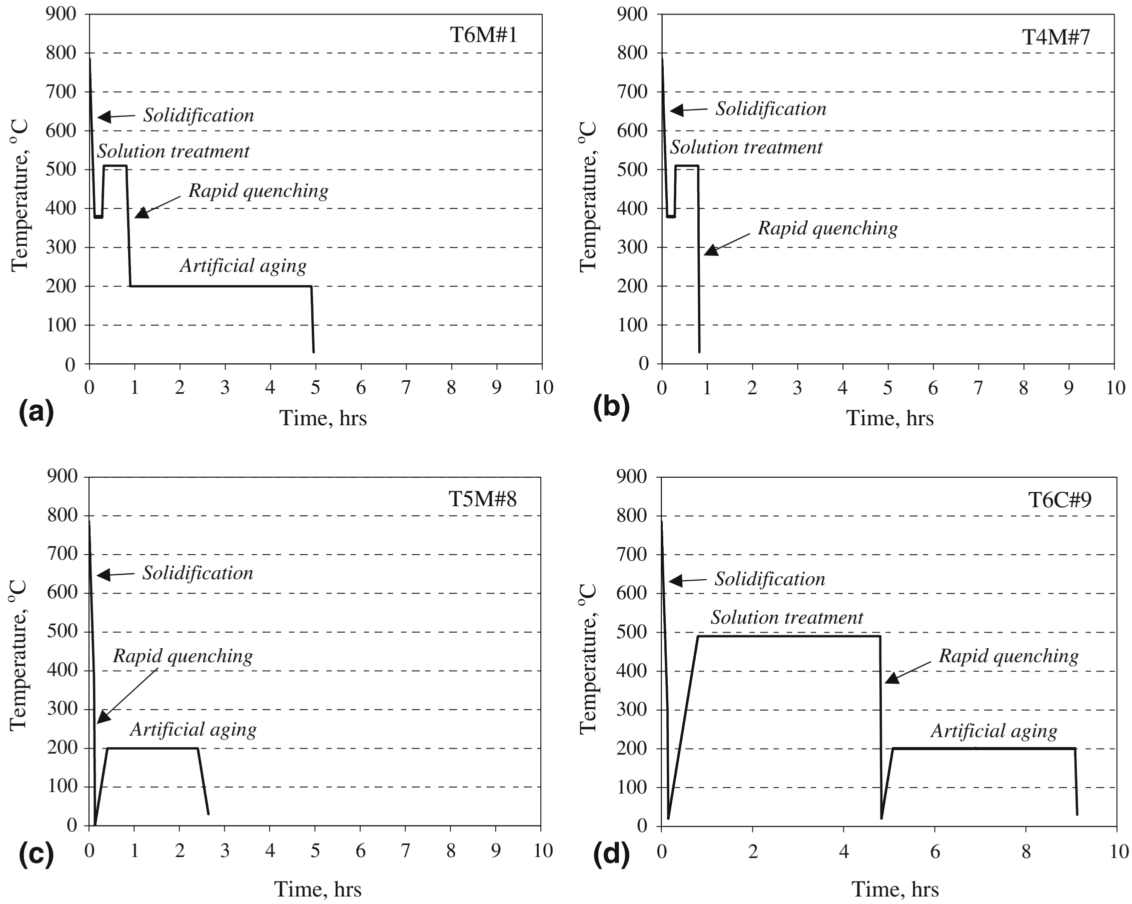

Fig. 6 Schematic temperature vs. time plots of the UMSA experiments for modified and conventional tempers performed for the Al-20%Si engine block and test samples. Table 2 provides complimentary experimental details. (a) T6 Modified—rapid solidification arrested at 380 °C, followed by solution at 510 °C for 0.5 h, air quenching and continuous aging at 200 °C for 4 h. (b) T4 Modified—rapid solidification arrested at 380 °C, followed by solution at 510 °C for 0.5 h, air quenching and the natural aging for 4 days. (c) T5 Modified—rapid solidification arrested at 380 °C, followed by the water quenching and aging at 200 °C for 2 h. (d) T6 Conventional—engine block solution at 490 °C for 4 h, air quenching and aging at 200 °C for 4 h

Table 2 Selected parameters of the UMSA experiments for modified and conventional tempers carried out for the Al-20%Si samples and engine block

Exp#	Temper	Temp. prior ST, °C	ST °C	ST h	Temp. after quench, °C	Quench rate, °C/s	Aging °C	Aging h	Total duration, h/min	Hardness, HRB
1	T6M	380	500	0.5	200	5	200	4.0	4/55	74.4 ± 1.3
2	T6M	380	500	4.0	200	5	200	4.0	8/15	76.8 ± 0.6
3	T6M	380	510	0.5	200	5	200	4.0	4/56	76.2 ± 1.3
4	T6M	380	510	4.0	200	5	200	4.0	8/16	75.9 ± 0.8
5	T6M	380	510	0.5	200	5	200	2.0	2/55	77.2 ± 0.7
6	T7M	380	510	0.5	240	5	240	0.5	1/31	69.2 ± 0.8
7	T4M	380	510	0.5	25	5	NA	96.0	0/41 (ST only)	73.6 ± 1.0
8	T5M		N/A	N/A	N/A	50	200	2.0	2/43	72.8 ± 1.4
9	T6C	RT	490	4.0	25	5	200	4.0	9/10	73.5 ± 1.7

Note: T4M-T7M—Modified tempers, ST—Solution Treatment, NA—Natural Aging for 4 days, T6C—Conventional T6 heat treatment for HPDC engine blocks, RT—Room Temperature, N/A—Not Applicable

2.5 Foundry Vacuum HPDC Trials and Heat Treatment Experiments

Foundry trials were carried out at the Yamaha Motors R&D facility in Japan using a Bühler 8MN cold chamber horizontal vacuum HPDC machine to cast linerless (monolithic) 250 cm^3 engine blocks (Fig. 1). Water cooled engine blocks are used for high performance motorcycle engines (Ref 4, 7). The weight of this engine block after the final machining operation was approximately 1.6 kg. The melt temperature in the holding furnace was kept at 785 °C and next was ladled into the HPDC machine shot sleeve and injected. The shot sleeve temperature before melt pouring was kept at approximately 200 °C. Time from the onset of injection to the completion of die filling was approximately 1.5 s. The die temperature, injection speed of the melt and lubricant were best selected to enable the mass production of this engine block. The gas content in the engine block was low (~0.3 cm^3/100 g) due to melt degassing and the vacuum-assisted die-casting process. The vacuum level during HPDC processing was approximately 200 mbars.

The engine block castings were water quenched right after their ejection from the HPDC cavity at approximately 380 °C. Test samples taken from the bore wall and thicker sections were used for microstructure evaluation including SEM/EDX and Image Analysis. The optical micrograph of the engine bore wall microstructure is presented in Fig. 2. The selected engine blocks were subjected to the conventional T6C#9 heat treatment performed under the following conditions: solution at 490 °C for 4 h followed by water quenching and by aging at 200 °C for 4 h (Table 2).

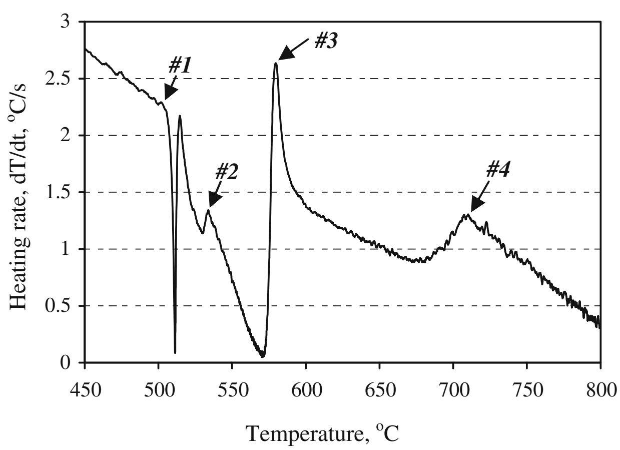

Fig. 7 First derivative (*dT/dt*) vs. temperature curve recorded for the ED = 50 µm test sample during the heating cycle to 785 °C with an average heating rate of 0.75 °C/s. The *numbered arrows* correspond to the following metallurgical reactions: #1—Beginning of the $AlCu_2$-based phase melting (non-equilibrium solidus temperature) (503.6 °C). #2—End of the Cu-, Mg-based phases melting (534.1 °C). #3—End of the Al-Si eutectic melting (580.2 °C). #4—End of the primary Si crystals melting (non-equilibrium liquidus temperature) (711.0 °C)

2.6 Microstructure Assessment and Hardness Measurements

All UMSA and foundry trial test samples taken from the bore wall and thicker sections were mounted in cold resin and the cross sections were prepared for metallographic observations. Hardness in the as-cast and in the heat treated conditions was measured using a Buehler Rockwell Tester (B scale, 100 kg load). Twenty (20) measurements (for each test sample) were made at a distance of 2 mm from the bore surface as shown in Fig. 8. Next, the average hardness and standard deviation were calculated and plotted. According to the Yamaha Motor Co. Ltd. engineering specifications, hardness as a quality indicator of the engine block bore section was chosen since it relates to the block's tribological characteristics. Therefore, hardness was selected as an indicator of the heat treatments' effectiveness.

An automated Leica Light Optical Microscope linked with the image analysis system was used for determination of the Equivalent Diameter (ED) of the primary Si particles. The ED was defined as the diameter of the circle having the same area as the analyzed feature. Twenty-five (25) analytical fields were analyzed and the average value of the ED and the corresponding standard deviation were calculated. The SDAS was measured by plotting the line across the dendrite arms. Next, the line length was divided by the number of intercepted dendrite arms. Thirty analytical fields were analyzed and the average values of the SDAS with corresponding standard deviation were calculated. Metallographic observations were made at 100× and 200× magnifications. The morphology of the primary and eutectic silicon as well as the intermetallic phases was analyzed with respect to the solidification conditions and parameters of the heat treatment processes.

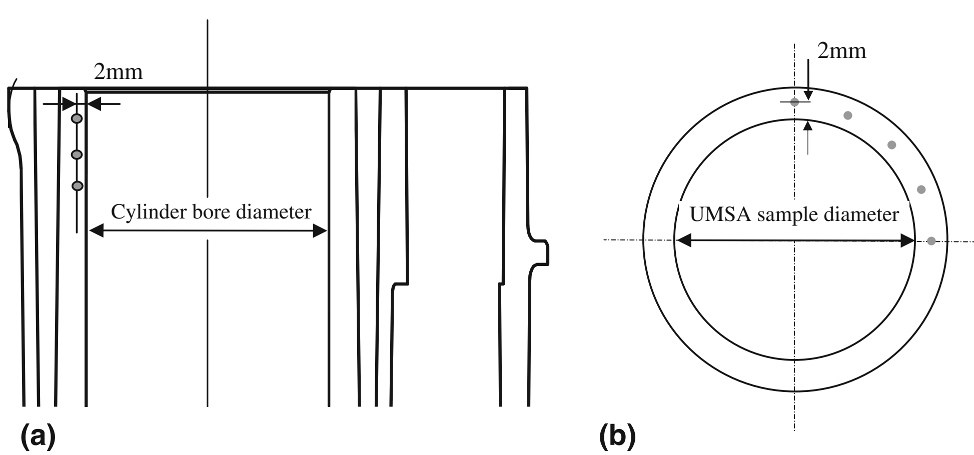

Fig. 8 Schematic illustration of the Rockwell (HRB) hardness measurements performed on the vacuum HPDC engine blocks and UMSA test samples. (a) Longitudinal section of the engine block with HRB indentations made 2 mm from the internal bore surface. (b) Cross section of the UMSA test sample with HRB indentations made at a distance of 2 mm from the internal sample surface

3. Results

3.1 The As-Cast Metallurgical Characteristics of the Al-20%Si Alloy Test Samples and Optimization of the Solution Treatment Parameters

Metallographic analysis showed that the as-cast microstructure of the UMSA test samples that solidified at a cooling rate of approximately 20 °C/s consisted of primary Si particles having an ED of approximately 50 µm (Fig. 5). The primary Si particles' size indicated satisfactory modification due to the combined thermal (high solidification rate) and chemical (phosphorus) mechanisms. SDAS of 13.6 ± 2.6 µm was predominantly a function of the cooling rate (Ref 2). The test samples also contained fine unmodified Al-Si eutectics, very fine Fe-based intermetallic and multi-elemental Cu, Mg, Si, and Al rich phases. The complex morphology of these multi-elemental phases is presented in Fig. 9(a). Mg, Si, and Al rich phases (darker gray) coexist with $AlCu_2$ particles (lighter gray). Dissolution kinetics of these phases during the subsequent solution treatment operation was crucial for the successful strengthening mechanism of the Al-20%Si engine block's aluminum matrix (Ref 4, 6, 23, 27).

The Thermal Analysis of the UMSA test samples subjected to the relatively rapid solidification process (Fig. 10) showed that the average cooling rate was approximately 20 °C/s while a maximum instantaneous cooling rate was reached at 45 °C/s. Previous work determined that the cylinder bore wall (thinner section that must provide excellent tribological characteristics, see Fig. 1) solidified at an average cooling rate that varied between 50 and 85 °C/s (Ref 2). The corresponding SDAS was within a range of 5-8 µm as indicated in Fig. 2. The observed microstructure variation was due to the solidification rate gradient across the bore wall. Satisfactory repeatability of the UMSA experiments and the resultant microstructural refinement level corresponded to both the thicker section and the cylinder bore section of the HPDC casting.

Precise determination of the non-equilibrium melting temperature of the tested samples is of paramount importance for development of energy and productivity efficient solution treatment procedures allowing for maximization of its temperature and elimination of the detrimental incipient melting of the AlCuMg-based phases. Thermal analysis of the ED = 50 µm test sample's heating cycle with an average rate of 0.75 °C/s revealed four (4) main metallurgical reactions (Fig. 7). It was found that the melting of the divorced $AlCu_2$ eutectic particles began at approximately 504 °C and the test sample melting process was completed at 711 °C which corresponds to the completion of the primary Si crystals melting. The convoluted #1 peak indicates that the multi-elemental Cu, Mg, Al, Si rich phase co-exists with the attached $AlCu_2$ particles as presented in Fig. 9 (Ref 3, 23, 25, 27). A heating rate greater than 0.2 °C/s combined with the 504 °C target solution treatment temperature in a single step could cause incipient melting of the AlCuMg-based phases (Ref 21, 26, 27). Previous studies indicated that the incipient melting temperature can be exceeded up to 10 °C by reducing the heating rate to the target solution temperature or by utilizing a two-step solution treatment process. It is known that slow heating rates help to dissolve some of the Cu-based phases before reaching the solution temperature (Ref 24). For this reason solution treatment optimization experiments were performed at 500 and 510 °C that was approximately 6 °C above the incipient melting temperature.

Metallographic observations of all heat treated test samples did not reveal any effect of the solution temperature and/or time on the primary Si crystals' size and distribution. This is due to high thermal stability of the primary Si crystals. Metallographic

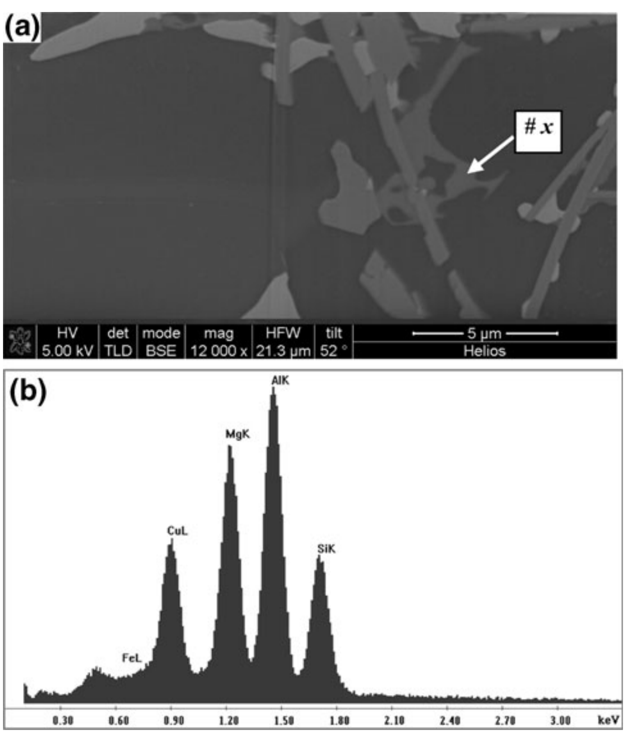

Fig. 9 Scanning electron microscope and energy dispersive x-ray (SEM/EDX) analysis results for the Al-20%Si vacuum as-cast HPDC engine block. (a) BSE micrograph of the very fine coexisting Cu, Mg, Al, and Si rich phases. Lighter gray—$AlCu_2$, darker gray—Al-, Mg-, Si-, Cu-based phase (Mag. 12000×). (b) X-ray microanalysis spectrum taken from spot (#x) of the darker gray phase indicates the presence of Al, Mg, Si, and Cu. Most likely the Cu peak was generated by the x-ray signal from the metal matrix

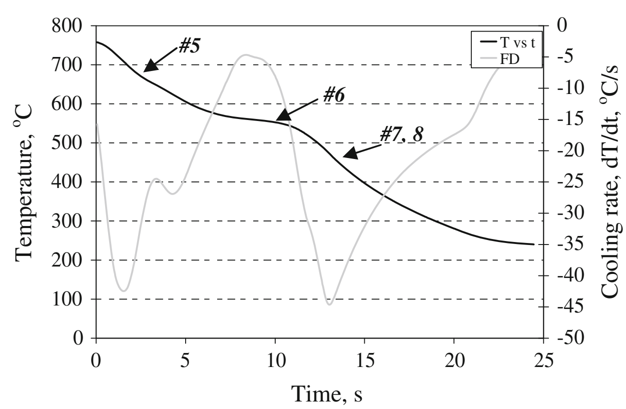

Fig. 10 Temperature vs. time (*T* vs. *t*) solidification curve and its first derivative (FD) curve for the Al-20%Si alloy, average cooling rate of approximately 20 °C/s (instantaneous up to 45 °C/s). The *arrows* correspond to the following metallurgical reactions: #5—Nucleation of the primary Si crystals. #6—Nucleation of the Al-Si eutectic. #7—Nucleation of the Cu-, Mg-, Al-, and Si-based phases. #8—End of the solidification process

observations revealed the lack of Al-Si eutectic modification of the test samples solution treated at 500 °C for 0.5 h (Fig. 11a). The microstructures seen in Fig. 11(b) to (d) predominantly showed the eutectic Si that underwent significant thermal modification for the analyzed solution treatment conditions. Considerable spheroidization of the eutectic Si particles was observed for test samples solution treated at 500 °C for 4 h (Fig. 11b). Silicon fragmentation and edge rounding were observed when the solution temperature was increased to 510 °C, while the treatment time was 0.5 h (Fig. 11c). These test samples were considered as partially modified. Increasing the solution temperature to 510 °C and time to 4 h resulted in subsequent uniform spheroidization of the eutectic Si particles having a diameter of up to 5 μm (Fig. 11d). The solution treatment performed at 510 °C was approximately 6 °C above the incipient melting temperature (504 °C) and did not cause any localized melting of the AlCuMg-based phases. The heating rate to the solution temperature was slow, i.e., 0.2 °C/s, and most likely partial dissolution of the soluble phases had already taken place before reaching the solution treatment temperature.

3.2 Hardness After Modified T6M, T7M, and T4M Heat Treatments

UMSA modified T6M solution treatment experiments 1 to 4 (Table 2, Fig. 12) were performed at 500 and 510 °C for 0.5 and 4 h and were carried out for the identical aging conditions at 200 °C for 4 h and represented the industrial processing used for the vacuum HPDC engine block. HRB hardness was increased up to 7.9 divisions as compared with the as-cast condition (68.9 ± 1.0) while the HRB range for samples 1 to 4 was between 74.4 and 76.8 divisions (Fig. 12). Experiments 1 to 4 rendered up to 3.3 divisions higher HRB in comparison with the heat treatment conventionally used for the vacuum HPDC engine blocks (73.5 ± 1.7 HRB). Solution treatment at 510 °C for 0.5 h and at 510 °C for 4 h rendered negligible HRB differences of 0.3 divisions; however, the heat treatment total duration can be reduced from approximately 8 to 5 h (Table 2). Solution treatment at 510 °C for 0.5 h and a total heat treatment duration of approximately 5 h rendered 2.7 divisions higher HRB values in comparison with the conventional

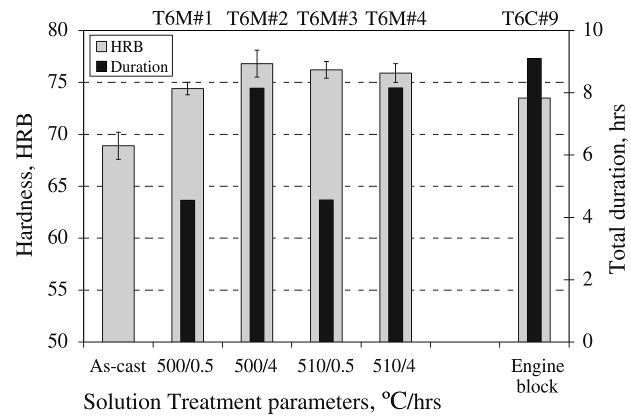

Fig. 12 Comparison of the as-cast engine block hardness and the effect of the solution treatment parameters on the hardness of the UMSA test samples and HPDC engine block subjected to solution treatment at 490 °C and aging at 200 °C for 4 h

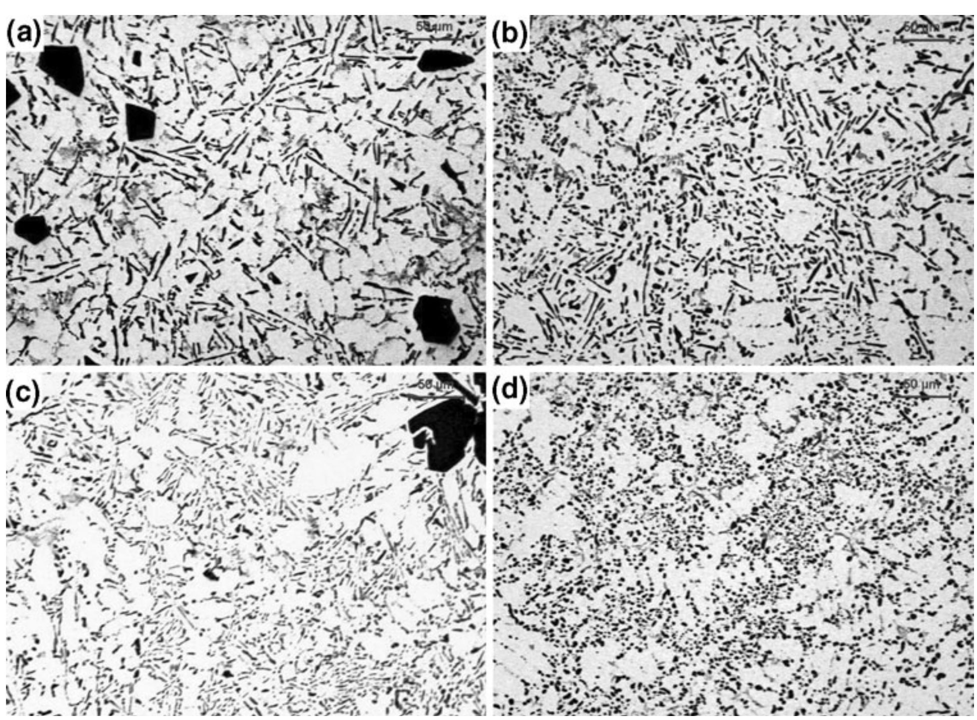

Fig. 11 Optical micrographs (200×) of the Al-20%Si phosphorus modified UMSA test samples showing predominantly eutectic Si (Primary Si crystals ED = 50 μm, Cooling rate = approximately 20 °C/s). At 380 °C the cooling process was arrested and test samples were subjected to the solution treatment operations followed by gas quenching and artificial aging at 200 °C for 4 h: (a) Solution at 500 °C for 0.5 h, (b) Solution at 500 °C for 4 h, (c) Solution at 510 °C for 0.5 h, and (d) Solution at 510 °C for 4 h

engine block solution treatment at 490 °C for 4 h with a total heat treatment duration of approximately 9 h (Fig. 12, Table 2). This significant time savings of 46% was achieved by utilization of a 20 °C higher solution treatment temperature.

UMSA experiments revealed that close integration of the solidification process with solution treating offered a potential 20-min reduction in overall processing time. Such "direct hot transfer" by arresting post-ejection casting cooling at 380 °C eliminates both the time and energy necessary for reheating of the component to the solution treatment temperature. Industrial-scale implementation of direct hot transfer poses significant practical shop floor challenges. However, die castings are produced incrementally in lots equal to the die cavity count, whereas heat treatment is typically performed in batches. Therefore, in order to maintain time-at-temperature needed to achieve identical thermal histories and optimum resultant properties for all parts—deployment of direct hot transfer theoretically drives manufacturing to a lot size of one. In addition, previous studies conducted by the authors also suggest that a higher direct hot transfer temperature increased casting hardness after solution treatment (Ref 27). Similarly, an additional 40 min of potential savings is possible by direct quenching from the solution to the aging temperature, again eliminating the time and energy necessary to reheat the casting to the prescribed aging temperature. Therefore, further study is required to optimize not only the technical potential of direct hot transfer, but the overall economics of a synchronous casting and heat treatment system.

Aging experiments for the T4M/#7 and T7M/#6 test samples (Table 2, Fig. 13) were subjected to the selected identical solution treatment operation at 510 °C for 0.5 h and subsequent gas quenching (5 °C/s) while aging parameters differed significantly. The T4M/#7 treatment involving the natural aging operation for 4 days rendered HRB of 73.6 that is 4.7 divisions higher as compared with the as-cast structure (68.9 ± 1.0 HRB) and is identical to the conventional T6C/#9 temper. However, the total duration for the T4M/#7 involved the solution treatment operation that took only 41 min in comparison with 9 h and 10 min for the T6C/#9. Thus, a savings of 92% in heat treatment duration involving necessary thermal energy was realized. The T7M#6 temper's artificial aging at 240 °C for 0.5 h resulted in HRB of 69.2 that is very similar to the as-cast one. Low hardness for the T7M#6 test sample relates to the high over aging temperature.

The modified T6M tempers (Table 2 experiments 3 and 5, Fig. 13) that included solution treatment at 510 °C for 0.5 h and artificial aging at 200 °C for 4 and 2 h resulted in increased hardness to 76.2 and 77.2 HRB, respectively. It was determined that for the modified T7M treatment with aging at 240 °C/0.5 h the hardness decreased to 69.2 ± 0.8 HRB caused by the over aging. Experimental results showed that the modified T4M, T6M, and T7M heat treatments increased the test sample hardness but it was done at the expense of a significant increase in process duration. Consequently, this approach will significantly raise manufacturing costs of the vacuum HPDC engine blocks.

3.3 Hardness After the Modified T5M Heat Treatment Experiments

The schematic temperature versus the time plot of the UMSA modified T5M experiment 8 is presented in Fig. 6(c). It was observed that for this temper (i.e., rapid solidification followed by water quenching from 380 °C and artificial aging at 200 °C for 2 h) the hardness was 72.8 HRB (Fig. 14, Table 2). This value was 4.4 divisions lower as compared with the modified T6M experiment 5 (77.2 HRB). It is interesting to observe that high temperature solution treatment has a major effect on the increased artificial aging structure's hardness and improvement of homogeneity expressed by the HRB standard deviation that is ±1.4 for T5M/#8, while ±0.7 for T6M/#5 for a comparable total temper duration of approximately 2 h 50 min.

Based on this observation, a less homogenous microstructure has to be expected for the HPDC castings in the T6C/#9 temper (solution at 490 °C for 4 h) as indicated by the higher standard deviation of ±1.7. However, the T6C/#9 temper delivers a finer structure with a higher level of homogeneity of the soluble $AlCu_2$ phases in comparison with the as-cast state showing the coarse and high volume fraction of undissolved

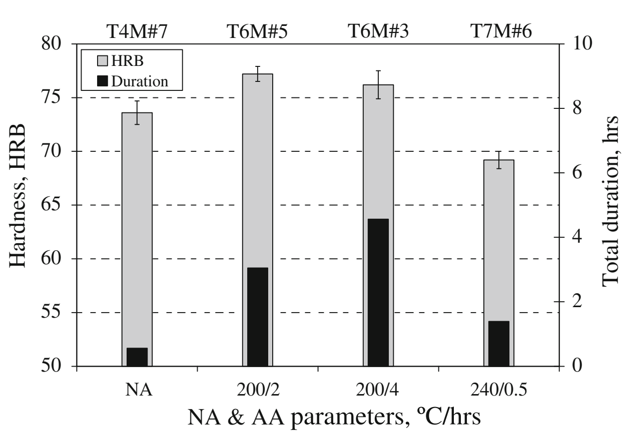

Fig. 13 The effect of the NA (Natural Aging) and AA (Artificial Aging) parameters on the hardness of the test samples subjected to the solution treatment at 510 °C for 0.5 h and various aging parameters. Please note that the total duration for the T4M#7 includes the solution time only since natural aging does not require furnace treatment

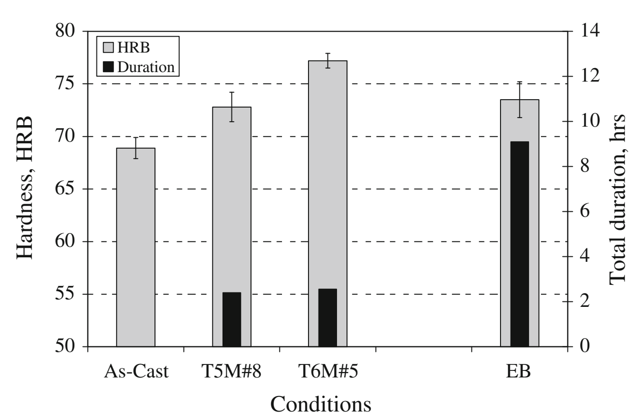

Fig. 14 Comparison of the as-cast hardness with the modified T5, T6, and engine block (EB) tempers hardness and total heat treatment duration. As-cast—Cooling rate: approximately 20 °C/s. T5 M/#8—Water quenching from 380 °C followed by aging at 200 °C for 2 h. T6 M/#5—Solution treatment at 510 °C for 0.5 h followed by gas quenching and aging at 200 °C for 2 h. EB—Solution treatment at 490 °C for 4 h followed by water quenching and aging at 200 °C for 4 h

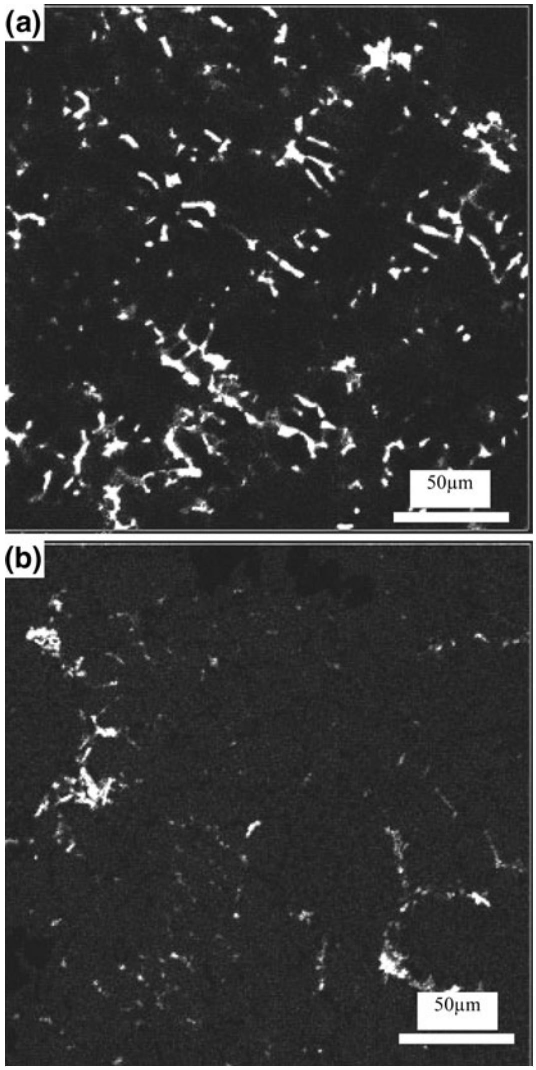

Fig. 15 Electron probe microanalysis maps of Cu-based phases in the vacuum HPDC engine block under the following conditions: (a) Solidified and water quenched at 380 °C, (b) Solution treatment at 490 °C for 4 h followed by water quenching

$AlCu_2$ phases; see Fig. 15 that shows the Electron Probe Microanalysis (EPMA) results.

It is worth pointing out that the test samples used for the modified T5M/#8 UMSA heat treatment experiments solidified at a rate of approximately 20 °C/s. This rate was between 2 and 4 times lower compared with the bore wall section of the vacuum HPDC engine block. Most likely the increase in the solidification rate will result in higher hardness following the solution treatment and artificial aging operations due to more effective retention of the solute atoms (Cu, Mg, and Si) in the metal matrix after solidification and solution treatment, and consequently a stronger precipitation effect during the aging process.

4. Discussion

The recent application of a vacuum-assisted HPDC technology considerably reduced the gas content in the cast components and consequently allowed for the subsequent high temperature solution treatment processing. An example of this technological approach is the state-of-the-art motorcycle linerless engine block made from hypereutectic Al-20%Si alloy (Fig. 1) (Ref 7). Thermal microstructure modification achieved by the rapidly solidified components resulted in the elevated as-cast mechanical properties and created a desired structure for subsequent energy efficient and high productivity heat treatment processing. Small SDAS (5-14 μm for cylinder bore and thicker sections, respectively) and a well refined Al-Si eutectic reduces the homogenization time required due to the reduced diffusion distances. The engine block's tribological properties to a large extent are controlled by the primary Si crystal size, distribution (Fig. 2) and its exposed height from the aluminum matrix. Proper design of the heat treatment operation increases the cast component's hardness and contributes to better tribological characteristics through the control of the Al-Si eutectic morphology, dissolution of the Cu- and Mg-based constituents and formation of the strengthening precipitates. In addition, heat treatment allows for control of the engine block's dimensional stability. Conversely, a poorly designed heat treatment increases the cast component's costs and does not contribute to the improvement of the HPDC component's performance.

Studies performed by Fuchs and Roósz (Ref 14, 15) indicated that for the Al-Si test sample containing 3 to 5% Cu and a SDAS of approximately 15 μm the solution time at 500 °C was between 15 and 30 min. When the SDAS was increased to approximately 55 μm, the calculated solution time was extended to approximately 2 to 4 h. Additionally, it is worth pointing out that the morphology of the Cu-based phases had an effect on its dissolution kinetics. The "blocky" $CuAl_2$ intermetallic phase (characteristic for slowly solidified castings) requires a longer solution treatment. A shorter solution time can be applied for the "fine eutectic" $CuAl_2$ phase morphology predominantly observed in rapidly solidified castings (Ref 23).

Selection of the engine block's thicker section microstructure for the heat treatment experiments will guarantee that thermal modification of the eutectic Si and the dissolution of intermetallics as well as significantly more effective precipitation kinetics will be achieved for the finer cylinder bore structure. The present work demonstrates the simultaneous fulfillment of the objectives to develop energy efficient solution treatment and artificial aging processes (short time duration) together with higher hardness (HRB = 75) than is presently being delivered by the conventional T6#9 temper (HRB = 73.5 ± 1.7). The presented heat treatment studies demonstrated the possibility for up to approximately 92% process time reduction as compared to conventional processing used for the vacuum HPDC engine blocks (T4M/#7, high temperature solution and natural aging versus T6C/#9, low temperature solution and artificial aging). The simplified T4M/#7 temper offers an identical HRB level as the T6C/#9 one (Fig. 12 to 14, Table 2). UMSA capabilities allowed obtaining a high level of repeatability and reproducibility for the solidification experiments (Ref 2, 3, 9, 26, 27, 29). In turn, this allowed for test samples with a predefined SDAS (representing specific casting sections) suitable for heat treatment processing. A rapid solidification of the Al-20%Si alloy test samples resulted in small SDAS and consequently more homogeneous distribution of the structural constituents within the interdendritic spaces and this minimized the diffusion distances and the time of the subsequent solution treatment. Optimization of the solution temperature (510 °C) maximized the effectiveness of the heat treatment. The exact determination of the alloy's melting temperature based on the thermal analysis of the solution treatment heating curve minimized the risk of incipient melting and improved the dissolution kinetics of the Cu- and Mg-based phases. In turn, this led to consequent process reduction time.

It is not unusual that the industrial solution temperature was determined based on the cooling curve analysis. Therefore, the metallurgical hysteresis effect (i.e., the difference between the non-equilibrium heating and cooling cycles' characteristic temperatures) could result in selection of ineffective parameters. For example, for the investigated Al-20%Si alloy the non-equilibrium solidus temperature during melting was approximately 504 °C. When measured during the solidification cycle it was approximately 480 °C. Neglecting the temperature hysteresis of 24 °C could lead to the selection of a significantly lower solution treatment temperature (Ref 3) and could result in negative consequences.

It was crucial to perform solution treatment at a maximum, but safe temperature, in order to avoid incipient melting (that could result in significant loss of casting mechanical properties) and reduce the processing time. The hardness of the high solution treatment temperature test samples was increased due to the elevated solid solubility of the Cu-, Mg-, and Si-based phases in the aluminum matrix. The solid solubility rate was increased by raising the solution treatment temperature. The low melting Cu, Mg, and Si rich phases were significantly decomposed through the dissolution process. Dissolution of the intermetallic phases was controlled by the diffusivity of the composing elements in the aluminum matrix and the phase curvature (interface mobility) (Ref 24, 26, 27).

Based on the studies performed for the 356 alloy by Shivkumar et al. (Ref 18) it was found that solution treatment at 500 °C could place approximately 0.5% Mg in solid solution. The concentration of Mg in the investigated Al-20%Si alloy was approximately 0.5% (Table 1) and its dissolution during the short solution treatment might be feasible. It can be pointed out that for the 356 alloy solution treated between 530 and 540 °C the dissolution was completed within 25 min for a permanent mold test bar and within 50 min for the sand cast test bars (Ref 18).

Current studies performed for the Al-20%Si alloy test sample(s) showed that the solution treatment could be performed a few degrees above the incipient melting temperature without risk of localized micro melting when partial dissolution of the well refined Cu, Mg, and Si rich phases takes place during a relatively slow heating rate. Industrial implementation of such energy efficient heat treatment schedules will require precise process control to avoid solution temperature overshooting.

The T5M/#8 temper could simplify the manufacturing process and reduce its duration by approximately 70%. If the HRB is approximately 73 this could be sufficient (Fig. 12 to 14, Table 2). This simplified thermal cycle consisted of water quenching after casting ejection from the die at approximately 380 °C followed by the artificial aging operation at 200 °C for 2 h (Fig. 6c). The premise for effective hardening during the T5M/#8 aging process was rapid casting solidification followed by water quenching from the predetermined temperature. The casting quenching rate has to be high enough to arrest the precipitation process from the saturated solid solution after completion of the solidification process. Results from this study indicated that rapid solidification combined with water quenching increased test sample hardness during the consecutive aging process by 3.9 divisions as compared with the as-cast condition (from 68.9 ± 1.0 to 72.8 ± 1.4 HRB). Elimination of the solution treatment and/or artificial aging operations has the potential to result in a significant cost savings. The T5M/#8 treatment requires 2 h and 43 min and renders HRB = 72.8 while the T4M/#7 temper duration is 41 min and renders HRB = 73.6. Therefore, the T4M is superior in this respect. However, some other aspects including engine block dimensional stability need to be investigated further since the T4-type tempers are the least dimensionally stable (tendency for precipitation in service). It will be necessary to develop the correlation between hardness and corresponding dimensional change over the lifetime of the engine's operation with respect to potential industrial application of the T4M temper. Moreover, some sections of the engine block are subjected to alternating loading conditions. Heat treatment may enhance fatigue performance by increasing casting hardness if detrimental features like porosity are minimized or eliminated. However, hardness variations during engine service for T4M/T5M heat treated castings could potentially have a negative effect on fatigue strength.

Heat treatment experiments resulted in an elevated Si level (Table 3) in the aluminum matrix of the vacuum HPDC engine blocks de-molded and water quenched at 380 °C as compared with the solution treated blocks at 490 °C for 4 h (Fig. 6d). Based on the x-ray microanalysis of the engine block samples it was determined that the Si weight concentration in the α aluminum matrix was $1.69 \pm 0.1\%$ and $0.57 \pm 0.01\%$, respectively (Table 3). These results corresponded to the observations by Kaczorowski and Szostak (Ref 16) for the Al-9%Si-Mg alloy that was cast using the permanent mold technology. It was concluded that higher hardness observed for water quenched castings was caused by matrix saturation by the Si atoms. In addition, it was reported that Si concentration exceeded the maximum solubility limit for the equilibrium conditions (1.79%Si) (Ref 16). The Cu concentration in the α aluminum matrix was increased from 0.76 ± 0.1 to $2.15 \pm 0.1\%$ for heat treated vacuum HPDC engine blocks as a result of the dissolution process during solution treatment at 490 °C. The x-ray microanalysis results were in good agreement with the Cu distribution images obtained using the EPMA technique (Fig. 15).

Table 3 Concentration of alloying elements in the α aluminum matrix obtained using electron probe microanalysis on the vacuum HPDC engine block test samples

Sample conditions	Concentration of alloying elements, wt. %			
	Cu	Mg	Si	Al
Solidified and water quenched at 380 °C	0.76 ± 0.1	0.14 ± 0.04	1.69 ± 0.1	97.41 ± 0.1
Solution treatment at 490 °C for 4 h and water quenched	2.15 ± 0.1	0.3 ± 0.0	0.57 ± 0.01	96.98 ± 0.1

The authors' preliminary results indicated that the possibility exists to further control casting hardness following the T5M/#8 heat treatment via optimization of the solidification process and the alloy's chemical composition. This could help to create conditions for favorable alloying elements distribution during the solidification process and consequently render a fine and homogeneous microstructure. The precise determination of the critical solidification rate and its impact on cast component aging response will be required. The extent of the casting segregation phenomenon could be minimized by adjusting the chemical modification of the intermetallic phases with respect to the casting solidification rate. Optimization of the Cu level for the Al-20%Si alloy would minimize the degree of segregation without compromising alloy hardness in the heat treated condition. It is known that the heat treatment parameters affect the amount of solute elements and consequently the precipitation strengthening process during the aging operation, the cast component's residual stress level and its dimensional stability. The optimum artificial aging process should ensure casting dimensional stability for the engine's operating conditions, a low residual stress level and a final hardness that will secure high tribological performance of the engine bore.

The experimental results obtained for the Al-20%Si engine block and for the UMSA test samples indicated that the modified T6M/#2 to 5 tempers (Table 2) increased HRB hardness up to 8.3 divisions as compared to the as-cast condition (HRB = 77.2 versus 68.9). The T6M/#5 temper (Table 2) that rendered the highest HRB of 77.2 was approximately 68% shorter in comparison with the duration of the T6#9 conventional temper that rendered HRB = 73.5.

The investigated Al-20%Si hypereutectic alloy is characterized by the high content of primary and eutectic Si that is predominantly responsible for the alloy's high hardness and consequently its good tribological characteristics. The strong contribution of Si phases (both primary and eutectic) to overall hardness could diminish the matrix hardness increase caused by the strengthening mechanism during the heat treatment operation.

Rising energy costs should provide a positive stimulus to revise the existing heat treatment standards—particularly for cast components that solidified under high solidification rates—paying careful attention to and taking great advantage of the thermal as-cast microstructure with its potential to leverage the metallurgical response of the component to subsequent heat treatment processing.

5. Results Summary and Conclusions

Based on the heat treatment studies carried out on the Al-20%Si linerless engine block and the UMSA test samples the following was concluded:

1. A solution treatment at 510 °C for 0.5 h followed by quenching and artificial aging at 200 °C for 2 h (T6M#5) resulted in a hardness of 77.2 HRB which is 3.7 divisions higher than the conventional T6C#9 currently used for the vacuum HPDC engine blocks.
2. The total process duration for the conventional T6C#9 temper (solution at 490 °C for 4 h and artificial aging at 200 °C for 4 h) is 9 h and 10 min, while the modified T6M#5 (solution at 510 °C for 0.5 h and aging at 200 °C for 2 h) has a total duration of 2 h and 55 min.
3. Considerable improvement of the hardness from HRB = 73.5 to 77.2 and the very significant reduction of the heat treatment duration of 68% was achieved due to the following parameters:

   – The solution temperature was increased from 490 to 510 °C without risk of incipient melting of the Cu-based phases.
   – The solution time at 510 °C was reduced from 4 to 0.5 h while exceeding the required hardness of 75 HRB and rendering significant thermal modification of the eutectic Si.
   – The aging time at 200 °C was reduced by 50% (from 4 to 2 h).

4. It is feasible to realize up to 92% savings in the heat treatment duration by utilizing the T4M/#7 parameters (solution treatment at 510 °C for 0.5 h and natural aging) instead of the conventional T6C/#9 temper (solution treatment at 490 °C for 4 h, artificial aging at 200 °C for 4 h). Both tempers rendered an identical HRB hardness of 73. The T4M/#7 solution treatment resulted in very good modification of the eutectic Si. Selection of the most appropriate temper parameters must take under consideration some other factors like dimensional stability of the heat treated cast component.
5. In the case where the acceptable cylinder bore hardness remains at the 73 HRB level then the modified T5M#8 temper could effectively be substituted by the T6M#5 modified temper resulting in additional savings in process duration. There is also the opportunity to further improve the T5M#9 temper's performance by increasing the quenching rate.
6. The UMSA test samples (SDAS = 13.6 μm) used for the heat treatment experiments represented the thicker section of the vacuum HPDC engine block's structure. Commercialization of the heat treatment optimization outcome for the thinner bore wall section (SDAS = 5-8 μm) will allow for further maximization of the casting hardness and will reduce process duration.

Acknowledgments

The authors would like to acknowledge the support of the Advanced Structural Materials for Next Generation Vehicles (ASM-NGV) Program of Natural Resources Canada as well as AUTO21, a member of the Networks of Centres of Excellence of Canada program. Moreover, the authors would like to thank Ms. Ellen Moosberger for her assistance with the preparation of this manuscript.

References

1. R.A. Legge, D.M. Smith, and G. Henkel, "Improved Aluminium Alloy for Engine Applications," SAE Paper No. 860558, 1986
2. H. Yamagata, W. Kasprzak, M. Aniolek, H. Kurita, and J.H. Sokolowski, The Effect of Average Cooling Rates on the Microstructure of the Al-20% Si High Pressure Die Casting Alloy used for Monolithic Cylinder Blocks, *J. Mater. Process. Technol.*, 2008, **203**, p 333–341
3. H. Yamagata, H. Kurita, M. Aniolek, W. Kasprzak, and J.H. Sokolowski, Thermal and Metallographic Characteristics of the

Al-20%Si High-Pressure Die-Casting Alloy for Monolithic Cylinder Blocks, *J. Mater. Process. Technol.*, 2008, **199**(1–3), p 84–90
4. H. Yamagata, *The Science and Technology of Materials in Automotive Engines*, Woodhead Publishing, Cambridge, 2005, p 37–38
5. N. Tenekedjiev and J.E. Gruzleski, Hypereutectic Aluminum-Silicon Casting Alloys—A Review, *Cast Met.*, 1990, **3**(2), p 96–105
6. J.E. Hatch, *Aluminum: Properties and Physical Metallurgy*, 3rd ed., American Society for Metals, Metals Park, OH, 1988, p 157–177
7. H. Kurita and H. Yamagata, Hypereutectic Al-20%Si Alloy Engine Block Using High-Pressure Die-Casting, *Proceedings of the SAE World Congress & Exhibition*, Detroit, USA, 2004-01-1028, 2004, PubMed
8. H. Yamagata and H. Kurita, "Effect of Elastic Deformation of the Honing Stone on the Exposure of Si-Crystals in a Hyper-Eutectic-Si Aluminum Cylinder Block," Society of Automotive Engineers of Japan, SAE International, 20056577, 2005
9. W. Kasprzak, J.H. Sokolowski, H. Yamagata, M. Sahoo, and H. Kurita, The Effect of the Melt Temperature and the Cooling Rate on the Microstructure of the Al-20%Si Alloy used for Monolithic Engine Blocks, *Int. J. Metalcasting*, 2009, Summer 09, p 55–71
10. M. Shamsuzzoha and F.R. Juretzko, Dual Refinement of Primary and Eutectic Silicon in Hyper-Eutectic Al-Si Alloys, *Aluminum Alloys for Transportation, Packaging, Aerospace and Other Applications*, 2007, p 153–162
11. G.K. Sigworth, Refinement of Hypereutectic Al-Si Alloys, *AFS Trans.*, 1987, **95**, p 303–314
12. H. Takagi, Y. Uetani, M. Dohi, T. Yamashita, K. Matsuda, and S. Ikeno, Effects of Mechanical Stirring and Vibration on the Microstructure of Hypereutectic Al-Si-Cu-Mg Alloy Billets, *Mater. Trans.*, 2007, **48**(5), p 960–966
13. S.N. Singh, B.P. Bardes, and M.C. Flemings, Solution Treatment of Cast Al-4.5%Cu Alloy, *Metall. Trans.*, 1970, **1**, p 1383–1388
14. E.G. Fuchs and A. Roósz, Time-Temperature-Dissolution (TTD) Diagrams for the Homogenization of As-Cast Structures in Al-Cu Alloys, *Z. Metallkunde*, 1972, **63**, p 211–214
15. E.G. Fuchs and A. Roósz, Comments on Solution Treatment of Cast Al-4.5%Cu Alloy, *Metall. Trans.*, 1972, **3**, p 1019–1020
16. M. Kaczorowski and R. Szostak, Influence of a Simplified Heat Treatment Method on the Structure and Properties of the Alloy AlSi9Mg, *Communications from the Institute for Forming, Welding and Foundry Technology*, Technical University, Warsaw, 1983, **59**(9)
17. D. Apelian, S. Shivkumar, and G. Sigworth, Fundamental Aspects of Heat Treatment of Cast Al-Si-Mg Alloys, *AFS Trans.*, 1989, **97**, p 727–742
18. S. Shivkumar, S. Ricci, B. Steenhoff, D. Apelian, and G. Sigworth, An Experimental Study to Optimize Heat Treatment of A356 Alloy, *AFS Trans.*, 1989, **97**, p 791–810
19. S. Shivkumar, S. Ricci, Jr., C. Keller, and D. Apelian, Effect of Solution Treatment Parameters on Tensile Properties of Cast Aluminum Alloys, *J. Heat Treat.*, 1990, **8**, p 63–70
20. N. Crowell and S. Shivkumar, Solution Treatment Effects in Cast Al-Si-Cu Alloys, *AFS Trans.*, 1995, **103**, p 721–726
21. J.H. Sokolowski, X.-C. Sun, G. Byczynski, D.O. Northwood, D.E. Penrod, R. Thomas, and A. Esseltine, The Removal of Copper-Phase Segregation and the Subsequent Improvement in Mechanical Properties of Cast 319 Aluminum Alloys by a Two-Stage Heat Treatment, *J. Mater. Process.*, 1995, **53**, p 385–392
22. A.I. Gracia-Celis, E. Velasco, S. Valtierra, J.F. Mojica, and R. Colas, Cooling Effect on Aging in a Cast Aluminum Alloy, *Automotive Alloys II*, San Antonio, Texas, USA, 1998, p 135–143
23. M.B. Djurdjevic, W. Kasprzak, C.A. Kierkus, W.T. Kierkus, and J.H. Sokolowski, Quantification of Cu Enriched Phases in Synthetic 3XX Aluminum Alloys Using the Thermal Analysis Technique, *AFS Trans.*, 2001, **16**, p 1–12
24. R. Fuoco and E.R. Correa, Incipient Melting During Solution Heat Treatment of an Al-Si-Mg and Al-Si-Cu-Mg Alloys, *AFS Trans.*, Paper No 02-135, *Transactions of the American Foundry Society and the One Hundred Sixth Annual Casting Congress*, Kansas City, MO, 4-7 May 2002, p 417–433
25. Z. Li, A.M. Samuel, F.H. Samuel, C. Ravindran, S. Valtierra, and H.W. Doty, Factors Affecting Dissolution of CuAl2 phase in 319 alloys, *Transactions of the American Foundry Society and the One Hundred Seventh Annual Castings Congress*, Milwaukee, WI, 2003, p 241–254
26. L.A. Dobrzanski, W. Kasprzak, and J.H. Sokolowski, Design Criteria used for Optimization of the Solution Treatment for 3xxx Series Cast Alloys, *13th Scientific International Conference Achievements in Mechanical and Materials Engineering AMME'2005*, Gliwice-Wisla, Poland, 2005, p 143–146
27. X. Chen, W. Kasprzak, and J.H. Sokolowski, Reduction of the Heat Treatment Process for Al-based Alloys by Utilization of Heat from the Solidification Process, *J. Mater. Process. Technol.*, 2006, **176**(1–3), p 24–31
28. M. Kasprzak, W. Kasprzak, W.T. Kierkus, and J.H. Sokolowski, "Method and Apparatus for Universal Metallurgical Simulation and Analysis," U.S. Patent No. 7,354,491, 2008, p 1–11
29. H. Onda, K. Sakurai, T. Masuta, K. Oikawa, K. Anzai, W. Kasprzak, and J.H. Sokolowski, *The Effect of Solidification Models on the Prediction Results of the Temperature Change of the Aluminum Cylinder Head Estimated by FDM Solidification Analysis*, Trans. Tech. Publications, Switzerland, Materials Science Forum, Vol 561–565, part 3, 2007, p 1967–1970